The Evaporative Demand Drought Index. Part II: CONUS-Wide Assessment against Common Drought Indicators

DANIEL J. MCEVOY,[a] JUSTIN L. HUNTINGTON,[a] MICHAEL T. HOBBINS,[b,c] ANDREW WOOD,[d] CHARLES MORTON,[a] MARTHA ANDERSON,[e] AND CHRISTOPHER HAIN[f]

[a] *Desert Research Institute, Reno, Nevada*
[b] *Cooperative Institute for Research in Environmental Sciences, University of Colorado Boulder, Boulder, Colorado*
[c] *NOAA/Earth Systems Research Laboratory/Physical Sciences Division, Boulder, Colorado*
[d] *National Center for Atmospheric Research, Boulder, Colorado*
[e] *Hydrology and Remote Sensing Laboratory, Agricultural Research Service, U.S. Department of Agriculture, Beltsville, Maryland*
[f] *Earth System Science Interdisciplinary Center, University of Maryland, College Park, College Park, Maryland*

(Manuscript received 22 July 2015, in final form 18 April 2016)

ABSTRACT

Precipitation, soil moisture, and air temperature are the most commonly used climate variables to monitor drought; however, other climatic factors such as solar radiation, wind speed, and humidity can be important drivers in the depletion of soil moisture and evolution and persistence of drought. This work assesses the Evaporative Demand Drought Index (EDDI) at multiple time scales for several hydroclimates as the second part of a two-part study. EDDI and individual evaporative demand components were examined as they relate to the dynamic evolution of flash drought over the central United States, characterization of hydrologic drought over the western United States, and comparison to commonly used drought metrics of the U.S. Drought Monitor (USDM), Standardized Precipitation Index (SPI), Standardized Soil Moisture Index (SSI), and the evaporative stress index (ESI). Two main advantages of EDDI over other drought indices are that it is independent of precipitation (similar to ESI) and it can be decomposed to identify the role individual evaporative drivers have on drought onset and persistence. At short time scales, spatial distributions and time series results illustrate that EDDI often indicates drought onset well in advance of the USDM, SPI, and SSI. Results illustrate the benefits of physically based evaporative demand estimates and demonstrate EDDI's utility and effectiveness in an easy-to-implement agricultural early warning and long-term hydrologic drought–monitoring tool with potential applications in seasonal forecasting and fire-weather monitoring.

1. Introduction

Drought is a complex and naturally occurring process with adverse effects on society, primarily through degradation and loss of agricultural crops and depletion of water resources (i.e., streamflow and reservoir storage). Recent examples are instructive: in California, the extended drought that began in late 2011 is still ongoing, and the 2011–14 three-year average precipitation (Prcp) record indicates that this period is the second driest in recorded history (Seager et al. 2015). In 2011, Texas experienced extreme Prcp deficits, while in 2011 and 2012 record-breaking air temperatures T_{air} and high wind speeds U played a significant role in drought intensification over much of the central United States (Karl et al. 2012; Cattiaux and Yiou 2013). Total economic losses are estimated to be $2.7 billion, $7.7 billion, and more than $35 billion for the California, Texas, and central U.S. droughts, respectively. While conditions in Texas deteriorated over many months in 2011, the depletion of moisture over the central United States in 2011 occurred at a much faster rate. This fast onset of drought has recently been termed "flash drought" (Svoboda et al. 2002). The physical mechanisms driving flash droughts have been largely neglected from traditional drought metrics. Hence, there is a growing need for continued development of physically based drought metrics that capture Prcp-independent land surface–atmosphere feedbacks, specifically the complementary relationship between actual evapotranspiration (ET) and atmospheric evaporative demand E_0.

Corresponding author address: Daniel J. McEvoy, Western Regional Climate Center, Desert Research Institute, 2215 Raggio Parkway, Reno, NV 89512.
E-mail: mcevoyd@dri.edu

DOI: 10.1175/JHM-D-15-0122.1

It has been common practice in recent decades to monitor and analyze drought using metrics driven by Prcp and T_{air} only. The two most commonly used drought indices are the Palmer drought severity index (PDSI; Palmer 1965), which relies on monthly T_{air} and Prcp, and the Standardized Precipitation Index (SPI; McKee et al. 1993), which relies on Prcp only. While the PDSI and SPI have proven useful for providing valuable information regarding hydrologic and meteorological drought, these metrics have limitations at short time scales and fail to account for the effects of other important meteorological and radiative forcings such as specific humidity q, U, and downwelling shortwave radiation R_d. The most heavily used dataset for decision-making with regards to drought is the U.S. Drought Monitor (USDM; Svoboda et al. 2002), which relies on a blend of metrics (including PDSI and SPI) and hydrologic data [e.g., soil moisture (SM), streamflow, and snow water equivalent] to produce weekly maps of drought severity. The USDM could be improved through the inclusion of important hydrometeorological forcings key to identifying flash and long-term drought through the use of physically based E_0 estimates.

Other operational products could similarly be improved with the inclusion of physically based E_0 estimates. For example, the U.S. operational PDSI, produced by the National Oceanic and Atmospheric Administration (Heddinghaus and Sabol 1991), continues to use T_{air}-based E_0 estimates (i.e., Thornthwaite 1948) within the PDSI formulation despite the fact that there have been a number of studies that recommend the use of physically based formulations of E_0 (e.g., Palmer 1965; Jensen 1973; Hobbins et al. 2008, 2012; Roderick et al. 2009; Milly and Dunne 2011; Hobbins 2016). Both Dai (2011) and van der Schrier et al. (2011) found PDSI to be largely insensitive to E_0 parameterization during the twentieth and early twenty-first centuries. On the other hand, Sheffield et al. (2012) found major differences between the PDSI driven with T_{air}-based and physically based E_0 estimates, especially from the mid-1990s through 2008, with T_{air}-based E_0 estimates showing a significant drying trend and physically based E_0 estimates indicating no significant trend in global drought severity. The role of physically based E_0 estimates in drought monitoring and prediction remains an active area of research and is a focus of this paper.

Recent studies have shown that ET, which is obtained through the use of thermal and optical satellite remote sensing or land surface models, used in combination with physically based E_0, can be used as a drought indicator by inherently accounting for feedbacks at the land surface–atmosphere interface through the use of ratios of ET to E_0 (Anderson et al. 2007a,b, 2011; Yao et al. 2010; Mu et al. 2013; Otkin et al. 2013, 2014). Evapotranspiration-based drought indices that use optical and thermal remote sensing, such as the evaporative stress index (ESI; Anderson et al. 2007a,b, 2011), have the advantage of being sensitive to rapid changes in soil moisture conditions that are driven by changes in the atmospheric drivers of T_{air}, U, q, and R_d and the unique ability to provide early warning of flash drought development (Otkin et al. 2013). Some of the limitations of using remotely sensed drought indices include cloud cover, satellite interarrival times that have to be interpolated, and limited record length for a robust climatology.

To complement indices like ESI, which estimate actual stress on the ground experienced by the vegetation, Hobbins et al. (2016, hereafter Part I) developed the Evaporative Demand Drought Index (EDDI), a measure of the drying potential of the atmosphere that can presage vegetative stress on the ground. Part I describes two primary physical feedbacks between ET and E_0 that form the rationale for EDDI: a complementary relationship under water-limited conditions (extended drought) where ET and E_0 vary in opposite directions (Bouchet 1963) and a parallel relationship under energy-limited conditions at the onset of flash drought. Under both scenarios, EDDI was found to respond to drying and wetting anomalies of major components of the hydrologic cycle (streamflow, ET, Prcp, and SM) at monthly to annual time scales in several river basins over the contiguous United States (CONUS) with different hydroclimates (Part I). At flash drought time scales (from weekly to monthly), increased E_0 (high EDDI) may not always lead to vegetative stress. To confirm drought stress, a thermal infrared–based remote sensing approach such as ESI can be useful.

This paper builds upon the work of Part I through a CONUS-wide assessment of EDDI against several commonly used drought indices. Data sources and methodology are presented first, followed by comparisons of EDDI to other commonly used drought metrics, flash drought case studies over the central and northeastern United States, and finally, extended drought case studies over the western United States.

2. Data and methods

a. Evaporative demand

Various methods have been developed to compute E_0, including T_{air}-based methods (e.g., Thornthwaite 1948; Hargreaves and Samani 1985), radiation-based methods (Priestley and Taylor 1972), and radiation–aerodynamic combination methods that incorporate maximum temperature T_{max}, minimum temperature T_{min}, R_d, U, and

q, such as the Penman–Monteith (PM) approach (Monteith 1965). A priori, it is generally assumed that if the necessary data resources are available, a full-form physically based method, such as PM, should be used over methods based only on T_{air} and/or radiation. Hobbins et al. (2012) and Hobbins (2016) demonstrated that the primary drivers of E_0 variability differ across the United States and with aggregation period (e.g., monthly vs annual) and season. For example, during summer months U is the primary driver of E_0 variability over much of the Great Basin, while R_d is the primary driver of variability over much of the southeastern United States. In this study, we use reference ET from the PM-based American Society of Civil Engineers standardized reference ET equation (Allen et al. 2005) for E_0. Daily bias-corrected and spatially disaggregated (from 12 to 4 km) gridded surface meteorological data (METDATA; Abatzoglou 2013) are used to compute E_0 on a daily basis for 1979–2015. Variables T_{max}, T_{min}, q at 2 m, R_d, and U [adjusted from 10 to 2 m following Allen et al. (2005)] were obtained from the University of Idaho (http://metdata.northwestknowledge.net/).

b. Evaporative Demand Drought Index

A probability-based standardized climate variable can be obtained using parametric or nonparametric methods. Parametric methods use a single probability distribution to fit a time series (e.g., Gamma distribution for SPI), where probabilities are transformed to standardized values through an inverse normal approximation. However, a single probability distribution may not always be appropriate at large spatial scales, and several studies have documented these limitations with SPI (Guttman 1999; Quiring 2009) and Standardized Streamflow Index (Vicente-Serrano et al. 2012). The EDDI calculation procedure is presented in Part I and uses a nonparametric probability-based approach to allow for more consistent comparisons between EDDI and other standardized indices.

The EDDI methodology follows Hao and AghaKouchak (2014), where the plotting position approach was used to compute SPI, Standardized Soil Moisture Index (SSI), and Multivariate Standardized Drought Index (MSDI). Farahmand and AghaKouchak (2015) recommend this plotting position approach to maintain consistency when comparing several standardized drought indices.

c. Comparison drought metrics

1) NLDAS-2-BASED DROUGHT INDICES

To assess the ability of EDDI to identify historical drought periods, EDDI is compared to SPI and SSI using Prcp and simulated SM from the North American Land Data Assimilation System phase 2 (NLDAS-2; Xia et al. 2012a,b). NLDAS-2 Prcp is primarily derived from Climate Prediction Center gridded daily gauge data [with a topographic adjustment from the Parameter-Elevation Regressions on Independent Slopes Model (PRISM; Daly et al. 1994)]. NLDAS-2 SM is derived from the Variable Infiltration Capacity model (VIC; Liang et al. 1994) and represents the average SM from the top 100 cm of the soil column. Daily NLDAS-2 data (Xia et al. 2012a,b) were provided (courtesy of Youlong Xia, NCEP) and used only for time series analysis of flash drought case studies (Fig. 8, described in greater detail below). Monthly NLDAS-2 data were obtained for the period of 1979–2013 with a native grid spacing of 0.125°. To compare EDDI to NLDAS-2 drought indices, all NLDAS-2 data were resampled to the 4-km (~1/16°) METDATA grid using bilinear interpolation. Precipitation and SM were accumulated at five time scales (1, 3, 6, 9, and 12 months) and standardized following the EDDI methodology of plotting positions and inverse normal approximation (Part I). Pearson linear correlation coefficients between EDDI and standardized NLDAS-2 drought indices were computed for each month (n = 35 years) at the five time scales.

2) EVAPORATIVE STRESS INDEX

The ESI (Anderson et al. 2007b, 2011) represents standardized anomalies in the ET fraction of reference ET (i.e., ET/E_0), with ET obtained through satellite-assisted modeling of the land surface energy balance. Evapotranspiration and other land surface energy balance components are retrieved using satellite optical and thermal imagery to force the Atmosphere–Land Exchange Inverse (ALEXI) surface energy balance model (Anderson et al. 1997, 2007a). Atmospheric variables needed to drive ALEXI come from the North American Regional Reanalysis (NARR; Mesinger et al. 2006).

Weekly ESI data were provided over the United States for 2000–13 at a 4-km spatial resolution and were aggregated to time scales of 1, 2, and 3 months. To obtain a consistent comparison between EDDI and ESI, EDDI was recalculated using the same period of record as the ESI (n = 14 years) and the same aggregation time scales. ESI data were resampled using bilinear interpolation to match the EDDI grid. No downscaling was necessary as both grids were of identical spatial resolution. Pearson linear correlation coefficients between EDDI and ESI were computed for each week over the 14-yr period and at all five time scales.

TABLE 1. Drought classes for comparing USDM to SPI, SSI, ESI, and EDDI. Positive EDDI values indicate drought with the upper percentiles (70–100) used to derive USDM classes.

USDM drought category	Description	SPI, SSI, and ESI percentiles	EDDI percentiles
*D*0	Abnormally dry	21–30	70–79
*D*1	Moderate drought	11–20	80–89
*D*2	Severe drought	6–10	90–94
*D*3	Extreme drought	3–5	95–97
*D*4	Exceptional drought	0–2	98–100

3) U.S. DROUGHT MONITOR

The USDM (Svoboda et al. 2002) was used as another metric to assess EDDI, with the primary goal of identifying differences between the two metrics during the evolution of drought through time and space. The USDM is derived from a blend of drought metrics adjusted using local expert knowledge to develop weekly drought severity maps over CONUS (Svoboda et al. 2002; Anderson et al. 2013). The USDM classification system of drought ranges from *D*0 (abnormally dry) to *D*4 (exceptional drought). For results where the USDM is compared, all drought metrics were converted to USDM classes (Table 1). The comparisons of EDDI to the USDM are necessarily qualitative because the USDM is a blend of information at several different time scales, whereas EDDI represents a single time scale.

USDM data (2000–13) were downloaded as Environmental Systems Research Institute, Inc. (ESRI), shapefiles provided by the National Drought Mitigation Center and rasterized to match the 4-km EDDI grid to create a USDM class map of integer values of drought intensity ranging from 0 to 4 (i.e., $D0 = 0$, $D1 = 1$, $D2 = 2$, $D3 = 3$, and $D4 = 4$).

3. Results

a. NLDAS-2 drought index correlations with EDDI

Temporal correlations r between EDDI and NLDAS-2 drought indices (EDDI–SPI and EDDI–SSI) for 1-, 6-, and 12-month time scales are shown in Fig. 1. Drought potential and drought itself are indicated by positive EDDI values and negative SPI and SSI values; therefore, strong negative correlations represent similar drought signals between EDDI and both SPI and SSI over the 35-yr period of record. At the 1–12-month time scales, correlations between EDDI and SPI and SSI are strongest (more negative) over much of the southwestern and south-central United States (with the exception of 1-month SSI), and highest in Texas ($r < -0.7$). The Northeast is a region of general weak correlations for both EDDI–SPI and EDDI–SSI, with the Midwestern states of Ohio, Indiana, and Michigan being a weak spot for EDDI–SPI only. Spatial correlations at 6- and 12-month time scales are quite similar (Figs. 1c–f) and are generally much stronger than at the 1-month time scale (Figs. 1a,b). Over the northeastern United States, EDDI–SPI correlations remain fairly weak at longer time scales, while EDDI–SSI correlations improve over Ohio, West Virginia, New York, and Pennsylvania (Figs. 1c–f).

Weak correlations to 1-month SSI over the western United States may be explained by above-average T_{air} and R_d (driving EDDI upward) that can lead to increased snowmelt and SM, and a short-term wetting signal from SSI, particularly during the winter months. Positive correlations of EDDI–SPI and EDDI–SSI over the northeastern United States are caused by energy-limited conditions, as opposed to water-limited conditions. In such regions, the rate of change in ET is generally proportional and in the same direction as E_0 (Han et al. 2014; Part I).

Figure 2 highlights four regions of interest selected for individual monthly correlation analysis. The Central Valley of California and Iowa are two major agricultural regions where drought impacts can have adverse effects on crop production. East-central Texas is part of a region that has been identified as a global ''hot spot'' for strong land surface–atmosphere coupling (Koster et al. 2004, 2006); therefore, strong correlation of SM and Prcp to EDDI is expected. Koster et al. (2009) identified Pennsylvania as an area where generally high SM exerts little control on ET because of prevailing energy-limiting conditions, even during times of severe meteorological drought. This observation is consistent with low correlations found in Fig. 1 in parts of the northeastern United States. The following section further highlights how E_0 anomalies (i.e., EDDI) in Pennsylvania relate to SM- and Prcp-driven droughts.

Individual monthly correlations between EDDI and NLDAS-2-derived indices at various time scales are shown in Fig. 3 for these regions of interest. For each of the selected regions shown in Fig. 2, EDDI correlations to SSI and SPI were area-averaged over all pixels. For

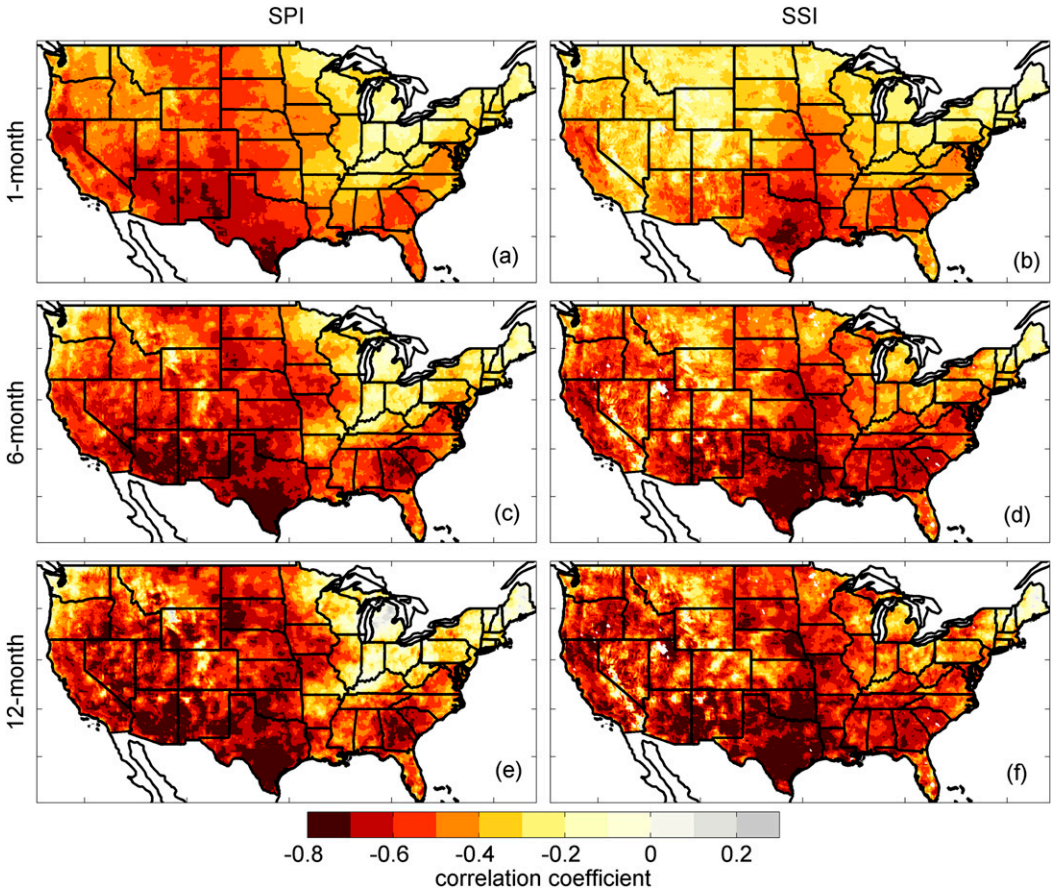

FIG. 1. Correlation coefficients between EDDI and SPI at (a) 1-month, (c) 6-month, and (e) 12-month time scales and between EDDI and SSI at (b) 1-month, (d) 6-month, and (f) 12-month time scales. Correlations were computed at each grid point for 1979–2013 over each month ($n = 35$) and then averaged over all months in each time scale.

the Texas region (Figs. 3a,e), seasonality and time scale had little impact on the strength of correlations and generally showed strong inverse relationships ($r < -0.6$ for SPI and $r < -0.7$ for SSI) during most months and time scales, supporting the conclusions of Koster et al. (2004, 2006).

For the California region, large seasonal and time scale–dependent variations were found, especially at the 1-month time scale for both SPI and SSI (Figs. 3b,f). Correlations ranged from +0.20 to −0.82, with the highest correlations occurring at the 6–12-month time scales during the growing season. An exceptionally weak correlation (−0.13) was found with SPI during July at the 1-month time scale. July is the driest month of the year for the Central Valley of California, and most Julys see zero Prcp accumulation. This limits the negative range of the 1-month SPI (McEvoy et al. 2012), causing poor correlations with EDDI. Furthermore, when it does rain during dry summer months, it occurs from isolated convective activity over a single day: even if most of the month is warm, cloud free, and dry (leading to a drought signal from EDDI), the SPI shows a wet anomaly. A more consistent stepped correlation pattern was revealed at longer time scales, where r values <-0.7 were found during the spring (April–June) for 3-month periods, spring and summer (July–September) for 6-month periods, and summer and fall (October–December) for 9- and 12-month periods.

Iowa was similar to Texas in that little variability was found in correlations (r values only ranged from −0.5 to −0.7), with the exception of the 1-month time scale. Lower correlations at 1-month time scales during the fall and winter should be expected with SSI, since the top 100 cm of ground is typically frozen during these months and land surface–atmosphere coupling is weak. There is a rapid increase in correlation at the 1-month time scale during the late spring and summer.

Correlations for the Pennsylvania region were the weakest of the four analyzed, with notably higher correlations to SSI (Fig. 3h) than to SPI (Fig. 3d). EDDI is

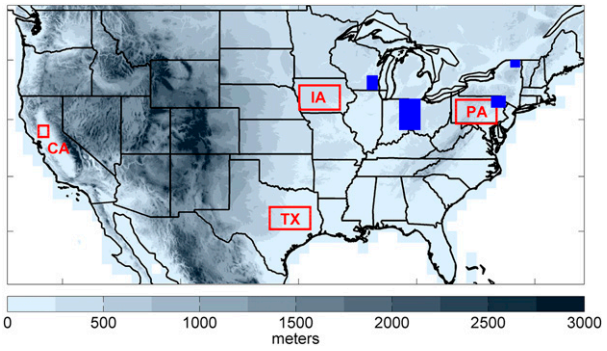

FIG. 2. Case study areas. Shading indicates METDATA terrain height (m) and red boxes indicate area-averaging domains for Fig. 3. Iowa (IA), Texas (TX), and Pennsylvania (PA) boxes are 50 × 100 4-km METDATA pixels (200 km × 400 km), and the California (CA) box is 25 × 25 pixels (100 km × 100 km). Blue patches indicate area-averaging domains for the flash drought cases in Fig. 8.

independent of Prcp and can be highly positive even during times of Prcp surplus. However, EDDI is not completely independent of SSI since changes in soil moisture are partially controlled by the drivers of physically based E_0. For SPI (Fig. 3d), r values never exceed −0.56, while for SSI (Fig. 3h) r values ranged from −0.60 to −0.69 during the summer and early fall at 1-, 3-, and 6-month time scales. Weak correlations were found to be both slightly positive and negative ($-0.30 < r < +0.20$) for SPI and SSI at the 1-month time scale during fall and winter, and for winter and spring months at other time scales. Results shown in Fig. 3 illustrate that EDDI may be particularly useful for flash drought and seasonal drought monitoring, especially during the growing season.

b. *ESI correlations with EDDI*

Seasonal temporal correlations between ESI and EDDI for CONUS are shown in Fig. 4. Only spring (April–June) and summer (July–September) periods are evaluated because of limited availability of continuous monthly ESI data during fall and winter. ESI data were frequently missing in snow-covered mountainous regions of the west during spring and summer periods, and ESI pixels were masked (indicated by white shading in Fig. 4, as in the mountain ranges of western United States) when less than 75% of the monthly time series was available over the period of 2000–13. One benefit of EDDI over ESI and other remote sensing–based metrics is that EDDI can be used during all seasons. This may be particularly useful for high-elevation hydrometeorological monitoring in seasonally snow-covered areas.

Figure 4 illustrates fairly large differences between spring and summer periods, with negligible differences between different time scales of 4, 8, and 12 weeks. During the spring period, negative correlations are strongest ($r < -0.7$) over much of Texas, the desert Southwest, and the Central Valley of California, while weaker relationships were found over the Northeast and parts of the Pacific Northwest (Figs. 4a,c,e). The low positive correlations in the Northeast are due to energy-limited evaporative conditions described in section 3a. Summer correlations (Figs. 4b,d,f) are strongest, and spatial patterns most consistent, over the central United States, and lower correlations are evident over parts of Nevada, California, and into the Pacific Northwest when compared to the spring period. Low summer correlations in Florida may be due to the shallow water table enhancing actual ET, and EDDI may not be a good indicator of drought potential in this region. Inspection of the summertime series from the regions of low correlation in the west and Pacific Northwest showed that, during certain summers, ESI and EDDI were strongly negatively correlated but positively correlated in others (not shown). Evapotranspiration rates in semiarid regions are typically low during summer periods; therefore, small variations in ET can potentially lead to large changes in ESI, making for poor correlations with EDDI. For example, most of Nevada experienced below-normal Prcp and high temperatures for July 2005, and EDDI and SPI indicated drought conditions, whereas ESI indicated wet conditions (not shown). In general, EDDI is strongly correlated to ESI ($r < -0.7$) during spring and summer months over much of the Southwest, south-central, and north-central United States.

c. *Flash drought during the growing season*

Flash drought can develop even during periods of normal or excess Prcp, and evaporative drivers can uniquely identify the onset and evolution of flash drought. For example, in some situations, a temperature-based E_0 would fail to identify rapid drying due to below-normal T_{air} coincident with high U and low q. The following highlights the Midwest droughts of 2011 and 2012 and several other case studies in the central and northeastern United States to demonstrate how EDDI can serve as an effective early warning of flash droughts.

Area-averaged time series of 1-month EDDI are compared to 1-month SPI and SSI during 2011 and 2012 in Fig. 5 for the Iowa domain. Note that the vertical axis of EDDI is inverted to better visualize drought onset and duration when compared to SPI and SSI in Fig. 5.

Figure 5 illustrates that in April 2011, all indices are near neutral (i.e., close to zero), and over the next 2 months EDDI changes to a moderate drought class (>0.78 or USDM $D1$ class), while both SPI and SSI increase to slightly wet conditions. SPI and SSI values

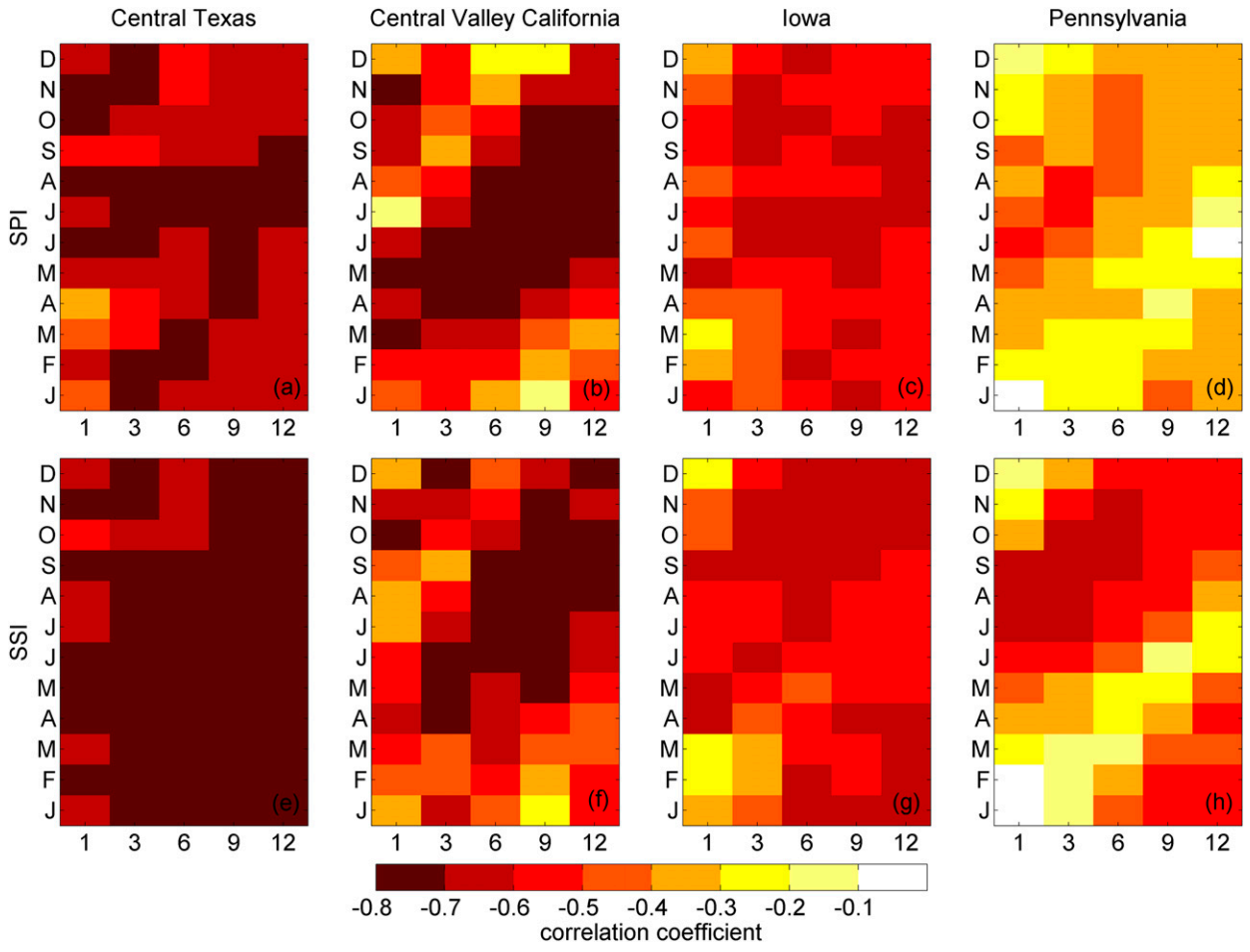

FIG. 3. Monthly correlations between (top) EDDI and SPI and (bottom) EDDI and SSI at all time scales for (a),(e) central Texas; (b),(f) the California Central Valley; (c),(g) Iowa; and (d),(h) Pennsylvania. The *y* axis indicates ending month of each time scale, and the *x* axis shows time scale (months). Shading indicates correlation coefficients. Correlations were computed at each grid point for 1979 to 2013 ($n = 35$) and then averaged over each climate region.

show no decrease until July 2011 (see black box in Fig. 5). EDDI reaches $D1$ in June, while SSI and SPI reach $D1$ in September, indicating a 3-month lead provided by EDDI. SPI falls below moderate drought in September, and SSI follows 1 month later in October. Both EDDI and SSI maintain extended drought conditions throughout all of 2012, with the exception of February, when EDDI is slightly above moderate drought (0.78), but still below zero. During this extended drought of 2012, SPI is highly variable and indicates wet conditions for many months.

To highlight the E_0 drivers that caused EDDI to signal first a flash drought and then an extended drought, a simple sensitivity analysis of EDDI was performed (Figs. 6a,b). For this analysis, E_0 was calculated while constraining the variable of interest to daily climatology values in order to isolate the impact of each forcing on the EDDI drought signal. Results are presented as estimates of EDDI with a notation of the variable of interest (i.e., EDDI-T, EDDI-q, EDDI-R_d, and EDDI-U). For example, EDDI-T was calculated using the daily climatology of T_{max} and T_{min}, and with METDATA-observed values for all other variables. During the period of 20–25 May 2011, EDDI-q and EDDI-U had the greatest separation from standard EDDI values in the negative direction (note *y* axis is inverted), which indicates that the drying power of the air term in the E_0 equation (U multiplied by vapor pressure deficit) initiated the flash drought signal in EDDI via increased U and below-normal q (Fig. 6b) during the period from 20 May through 5 June. In this case, using daily climatology q and U values mitigated the drought signal relative to the standard EDDI. By June 2011, EDDI decreased below the moderate drought threshold (0.78), with the primary difference from May being that U and T_{air} were then acting in combination to exacerbate the

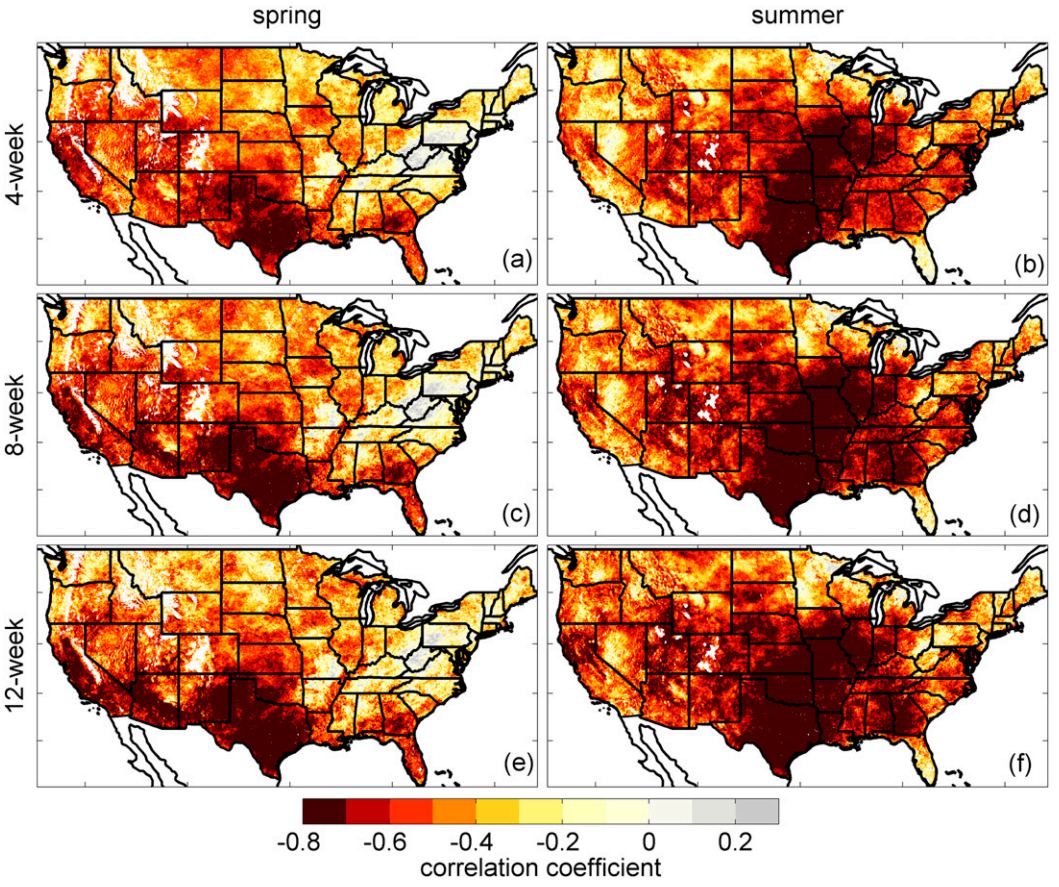

FIG. 4. Seasonal (April–September) correlation coefficients [(left) spring and (right) summer] between ESI and EDDI at (a),(b) 4-week; (c),(d) 8-week; and (e),(f) 12-week time scales. Areas in white indicate an insufficient amount of ESI data. Correlations were computed at each grid point for 2000–13 over each week (n = 14 years) and then averaged over all months.

drought signal—as opposed to T_{air} moderating it in May. Despite below-normal T_{air} conditions in September 2011 (Fig. 6a), the standard EDDI drought signal was maintained because of extremely low q values evidenced by a large difference between EDDI and EDDI-q (absolute difference of 1.17). From November 2011 through May 2012, T_{air} dominated the EDDI signal, as seen by the large differences between EDDI and EDDI-T. This increase in T_{air} and E_0 likely contributed to the persistent SSI drought signal throughout 2012, despite above-normal Prcp for February, April, October, and December (see Fig. 5).

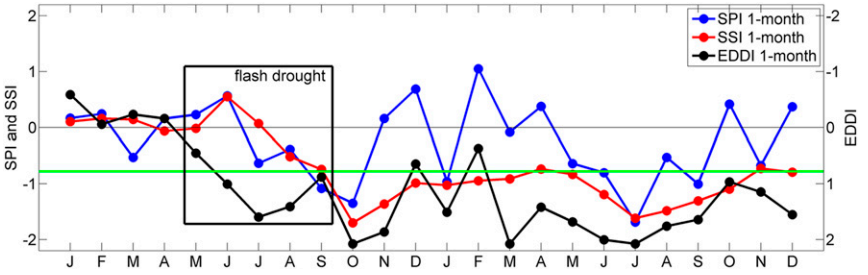

FIG. 5. EDDI under sustained and flash drought conditions. Monthly time series of 1-month EDDI, SSI, and SPI area averaged over the Iowa domain for 2011 and 2012. Note that the y axis of EDDI is inverted to clearly visualize drought onset and duration relative to SPI and SSI. Light green reference line indicates start of moderate drought classification (EDDI = 0.78, SPI and SSI = −0.78).

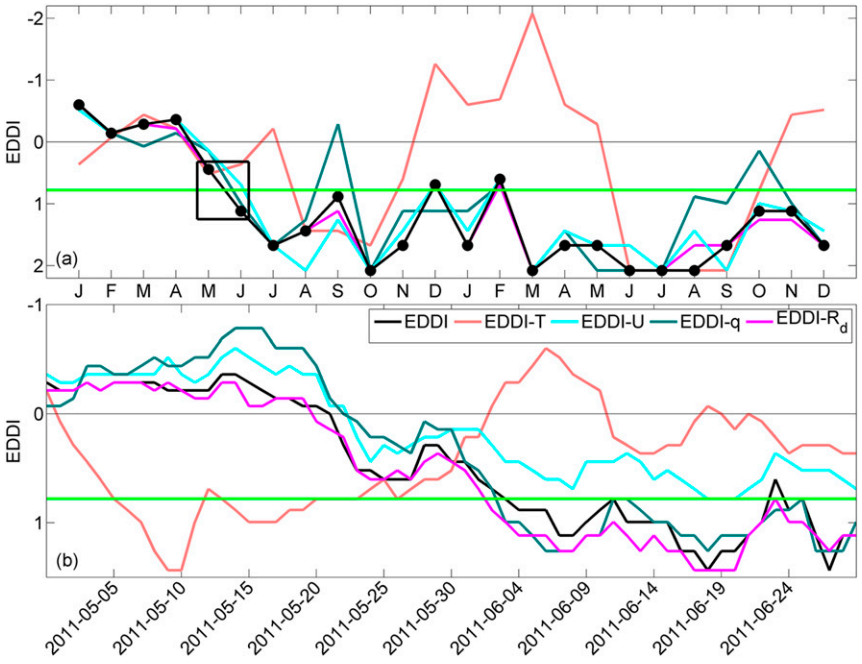

FIG. 6. (a) Monthly time series (values on the last day of each month) of 1-month EDDI and EDDI constrained by climatology T_{air} (EDDI-T), q (EDDI-q), R_d (EDDI-R_d), and U (EDDI-U) for 2011 and 2012. Black box highlights time period shown in (b). (b) Daily time series of 1-month EDDI, EDDI-T, EDDI-q, EDDI-R_d and EDDI-U for May and June 2011 shown to highlight details of flash drought initiation. Each day in the time series uses the previous 30-day accumulated E_0. Note that the y axis of EDDI is inverted. Light green reference line indicates start of moderate drought classification (EDDI = 0.78).

To spatially assess EDDI during the 2012 drought, a comparison was made between the USDM, SPI, SSI, and ESI. Recall from section 2e that the USDM is a blend of products at various time scales, but we are comparing it here to a fixed time scale EDDI: thus, the EDDI and the USDM distributions should not be expected to be identical. The objective of the EDDI and USDM comparisons is to show that EDDI can presage rapid onset droughts before the impacts show up in the USDM, thus highlighting the substantial added value gained by using EDDI in conjunction with other drought-monitoring metrics for decision-making applications.

Figure 7 shows the evolution of the 1-month EDDI, ESI, SSI, and SPI, and USDM through time and space over the spring and summer of 2012. The USDM generally indicated no drought or only $D1$–$D2$ over much of the central United States as of 1 May (Fig. 7a). In contrast, EDDI indicates at least moderate drought conditions over most of the same region and looks similar to the USDM spatial distribution of 2 months later (i.e., of 3 July 2012). EDDI responded to anomalously high T_{air}, U, and R_d across the region during the second half of April. ESI showed widespread neutral conditions for April with a rapid intensification in May. SSI and SPI show a slower progression and more local intensification (nonuniform spatial distribution) when compared to EDDI and ESI. The 2012 drought evolution illustrated by the USDM over the central United States expands in both spatial extent and severity throughout the summer; however, the progression from $D0$ to $D3$ and $D4$ takes approximately 3 months. Figure 7 illustrates that 1-month EDDI presaged the onset of USDM extreme to exceptional drought ($D3$–$D4$) by as much as 2 months. This case study highlights the application of using EDDI to identify future drought potential and onset of drought.

Four additional flash drought cases from Pennsylvania, New York, Wisconsin, and the Ohio–Indiana border are presented in Fig. 8 using daily time series of 1-month EDDI, SPI, and SSI during the growing season (April–September). Two of these cases (Wisconsin 2002 and Ohio–Indiana 2007) are examples from Otkin et al. (2014). Two new cases (Pennsylvania 1983 and New York 1991) are presented in this study to show that EDDI is effective in energy-limited regions such as Pennsylvania, despite low correlations to SPI there (see Fig. 3d). All four case studies are located in major agricultural regions. Domains used for spatial averaging

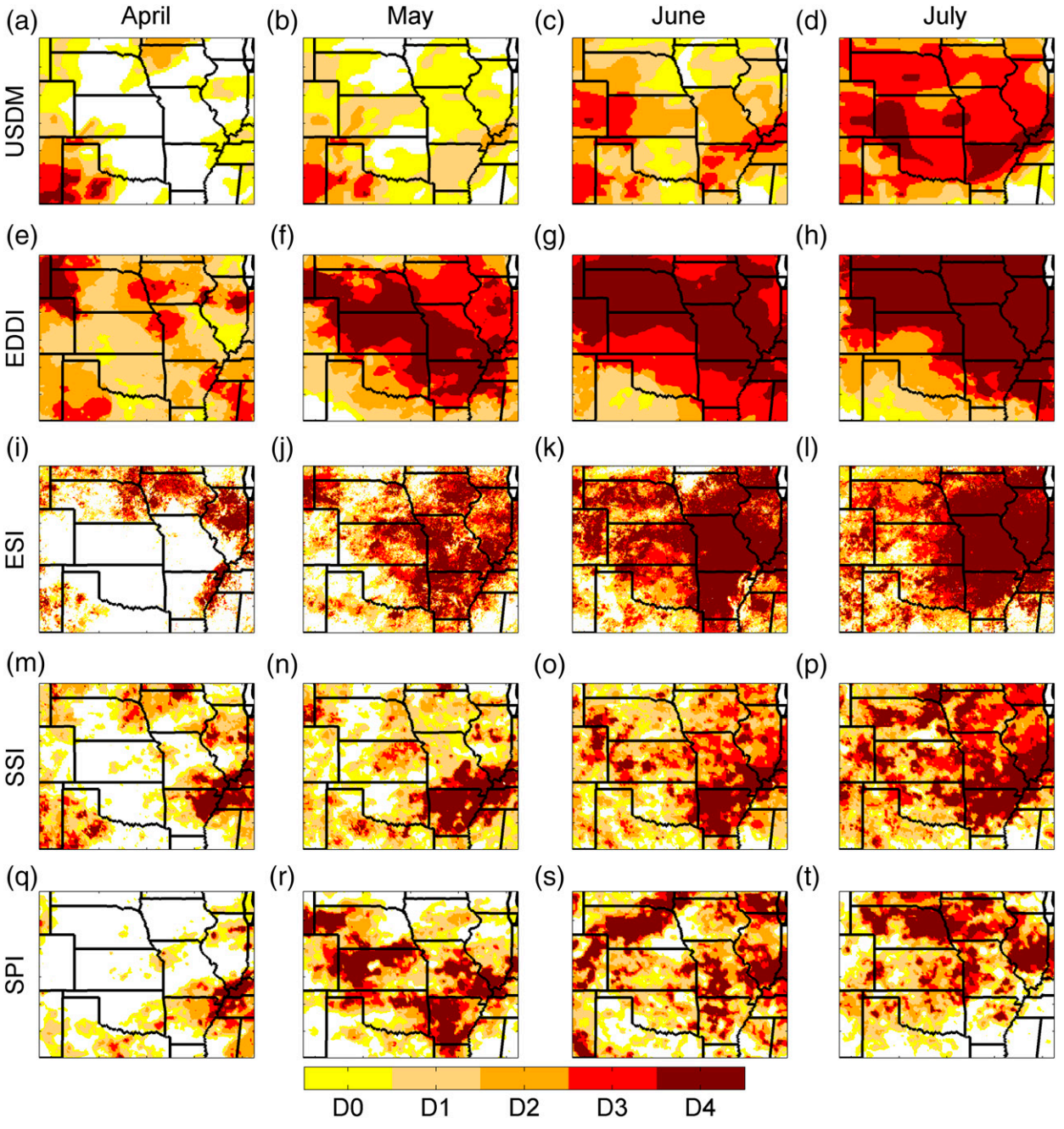

FIG. 7. Evolution of (from top to bottom) the USDM, 1-month EDDI, 1-month ESI, 1-month SSI, and 1-month SPI through the spring and summer of 2012. USDM data are from (a) 1 May, (b) 5 Jun, (c) 3 Jul, and (d) 31 Jul 2012. (e)–(h) EDDI, (i)–(l) ESI, (m)–(p) SSI, and (q)–(t) SPI are at 1-month time scales at the end of each month. All drought metrics have been converted to USDM categories according to Table 1.

are presented in Fig. 2. For the Pennsylvania case, EDDI decays rapidly from neutral to severe drought in 10 days starting around day 180. At the same time, there is a rapid spike in SPI to moderate wetness and then a slow decline toward drought and another rapid decline from days 206 to 210. Both EDDI and SPI converge on extreme drought at day 210, while the slower-to-respond SSI never reaches the extreme drought criterion. This type of signal, where EDDI shows a rapid change and SPI and SSI slowly move toward drought, could be used as a warning signal for potential on-the-ground drought impacts. For the New York case, both EDDI and SPI

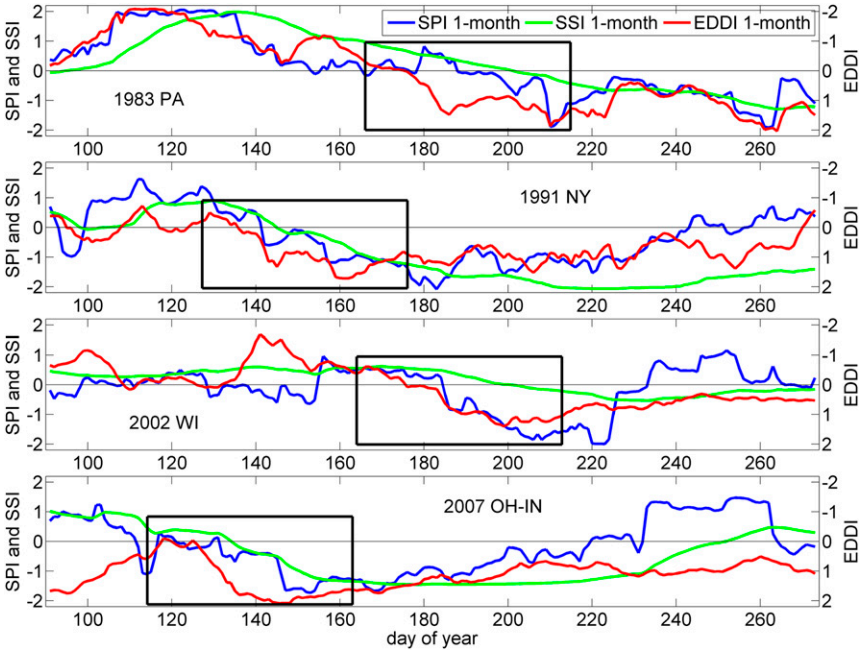

FIG. 8. Flash drought case studies using daily time series of 1-month EDDI (red line), 1-month SPI (blue line), and 1-month SSI (green line). Note that the *y* axis of EDDI is inverted to clearly visualize drought relative to SPI and SSI. Averaging domains are shown as blue patches in Fig. 2 and include (from top to bottom) Pennsylvania, New York, Wisconsin, and Ohio–Indiana. Black boxes highlight the periods of flash drought.

show two distinct rapid declines, the first at day 140 and the second at days 156 (SPI) and 157 (EDDI), with EDDI reaching drought threshold prior to SPI. The EDDI drought peaks about day 160, SPI at 180, and SSI around 220. For Wisconsin, EDDI and SPI are closely correlated during the onset of drought, but SPI maintains a longer and more severe drought. The Ohio–Indiana case is similar to the Pennsylvania case in that EDDI shows the flash drought (starting at day 128) well in advance of the crash of SPI that starts at day 145. In all four cases, EDDI is able to detect the flash drought prior to, or at the same time as, SPI and always ahead of the SSI signal.

Results illustrated in Figs. 5–8 of this paper and in the companion paper (Part I) highlight two major focal points of this research: 1) EDDI is a leading indicator of flash drought conditions and 2) a physically based E_0 is required to capture this signal. This reinforces the work of Hobbins et al. (2012) and Hobbins (2016), who concluded that T_{air} is not always the dominant driver of E_0 and that temperature-based parameterizations could lead to false drying (or wetting) signals when used for drought-monitoring applications. Our findings (illustrated in Fig. 5) also contradict the notion that 2012 should be considered a flash drought case over central Iowa [in contrast to Mo and Lettenmaier (2015)]: our results clearly indicate a well-established and persistent drought signal by both EDDI and SSI, with SPI being the only indicator to signal a rapid transition from wet to dry over the period of April–July. Figure 5 illustrates that the flash drought signal appeared in EDDI starting in May 2011 and in SPI and SSI starting in August 2011.

d. Extended drought in arid to semiarid regions

In this section, we examine whether EDDI can be used to characterize historical extended droughts over the western United States. Droughts in arid to semiarid regions of the United States are generally slower to develop than in the central United States, primarily because of the manner in which water resources are both naturally and anthropogenically stored. Natural water storage occurs as winter snowpack at high elevations that typically reach maximum depth in March or April. During spring and summer snowmelt, runoff is stored in reservoirs. Hydrologic drought severity in the west is strongly linked to reservoir storage and streamflow (McEvoy et al. 2012; Abatzoglou et al. 2014).

Four extended drought case studies using the USDM, EDDI, SPI, and SSI are shown in Fig. 9. The first case focuses on the extreme southwestern drought of 2002 (Figs. 9a,e,i,m), with the USDM mapped on 25 June 2002 (Fig. 9a) and the 6-month EDDI, SPI, and SSI

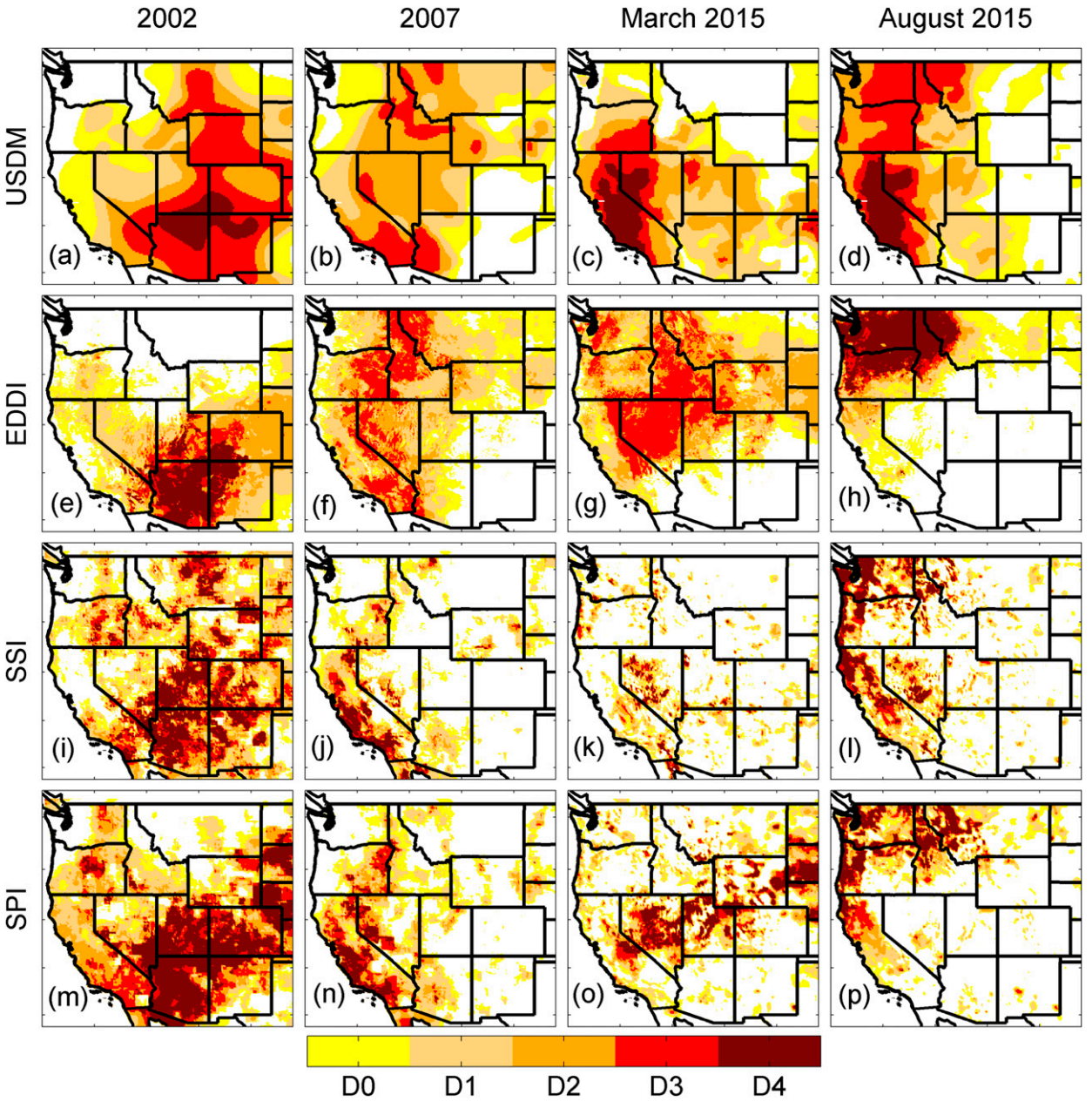

FIG. 9. Spatial comparison of drought metrics across the western United States. (a)–(d) USDM on 25 Jun 2002, 2 Oct 2007, 31 Mar 2015, and 1 Sep 2015; (e)–(h) 6-month EDDI in June 2002, 12-month EDDI in September 2007, 6-month EDDI in March 2015, and 6-month EDDI in August 2015; (i)–(l) 6-month SSI in June 2002, 12-month SSI in September 2007, 6-month SSI in March 2015, and 6-month SSI in August 2015; and (m)–(p) 6-month SPI in June 2002, 12-month SPI in September 2007, 6-month SPI in March 2015, and 6-month SPI in August 2015.

mapped for January–June 2002 (Figs. 9e,i,m). All metrics show a similar spatial structure of drought extent, although EDDI and SPI indicate little to no drought in Montana. Temperatures were lower than normal over much of Montana, Wyoming, and the northern portions of Utah and Colorado and slightly above normal for the Four Corners region (not shown). This indicates that T_{air} was likely driving EDDI negative in Montana; however, T_{air}, q, and U must have all played a role in driving EDDI in the positive direction over Utah and Colorado.

The second case focuses on the drought of the 2007 water year (from October 2006 through September 2007; Figs. 9b,f,j,n). The USDM on 2 October 2007 indicates 78% (percent area) of the western United States

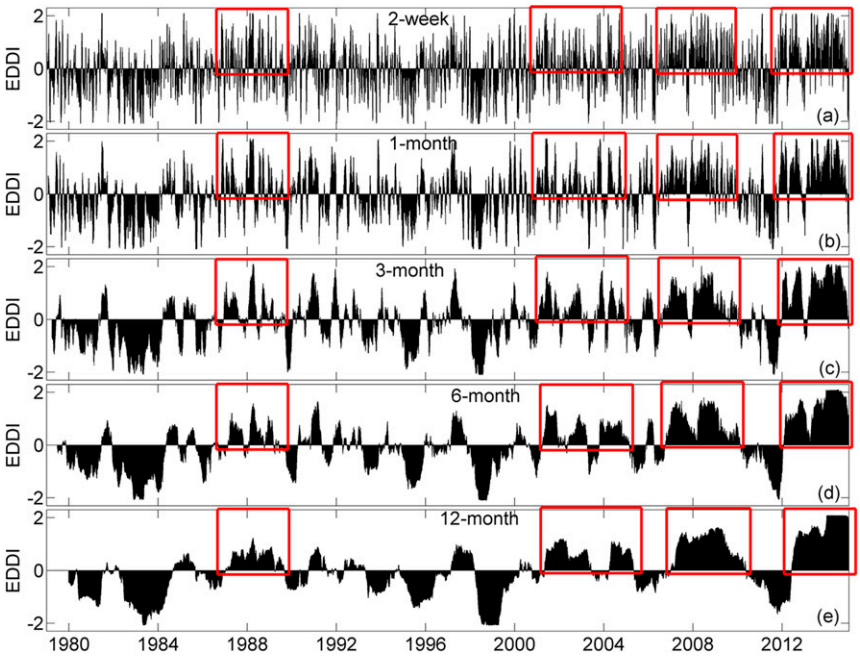

FIG. 10. Area-averaged time series of EDDI over the northern Sierra Nevada from 1979 to 2014 aggregated at (a) 2-week, (b) 1-month, (c) 3-month, (d) 6-month, and (e) 12-month time scales. Red boxes highlight the four most prominent hydrologic droughts during the time period.

in at least *D*0 (Fig. 9b). Figure 9f illustrates the 12-month EDDI ending in September 2007 and has the strongest spatial coherence and severity when compared to the USDM, while SSI and SPI (Figs. 9j,n) underrepresent the spatial extent shown by USDM and EDDI, particularly over Nevada, Idaho, and western Montana.

The third case highlights the extraordinary snow drought that occurred during the winter of 2014/15 (Figs. 9c,g,k,o). At the end of March 2015, the USDM continued to show *D*3 and *D*4 over much of California and Nevada, but little to no drought over the Washington Cascades and northern Rockies of Idaho and Montana (Fig. 9c). The period from October 2014 through March 2015 saw near-normal or even slightly above normal Prcp over much of the Pacific Northwest, which is reflected in the 6-month SSI (Fig. 9k) and SPI (Fig. 9o). However, record warmth during this period led to extremely freezing levels and much of the Cascade Range measured snowpacks of less than 25% of normal by the end of March (not shown). Record warmth and lack of Prcp led to similar snowpack conditions over the Sierra Nevada. The 6-month EDDI is the only indicator to reflect the snow drought conditions in the Cascades and northern Rockies (Fig. 9g). The fourth case (Figs. 9d,h,l,p) shows that by the end of August 2015, the USDM showed Washington 100% covered by *D*2 (13.36%) and *D*3 (86.64%), with widespread *D*3 over northern Idaho and western Montana (Fig. 9d). Six-month EDDI (Fig. 9h), SSI (Fig. 9l), and SPI (Fig. 9p) all agree at this point and show widespread *D*3 and *D*4 over the Cascades, northern Idaho, and Montana. The summer of 2015 was a devastating wildfire season for California and much of the Pacific Northwest, with close to 10 million acres burned in the United States (National Interagency Fire Center; https://www.nifc.gov/fireInfo/fireInfo_stats_totalFires.html), a result of the snow drought and record winter warmth followed by a hot and dry summer. The third and fourth cases (Figs. 9g,h) demonstrate that EDDI is not only a drought indicator but that it can also potentially serve as a wildfire risk indicator. Further research on relationships between EDDI and wildfire risk will be conducted in future studies.

The potential usefulness of EDDI to aid in the interpretation of hydroclimatic states at multiple time scales and over long time periods is assessed in Fig. 10, which illustrates time series of EDDI averaged over the northern Sierra Nevada for 1979–2014. As the northern Sierra Nevada provides much of the water resources to western Nevada and California, the use of multiple complementary drought metrics for evaluating short and extended drought in this region is invaluable. EDDI at the 2-week and 1-month time scales (Figs. 10a,b) closely correspond to documented heat waves and

extreme fire weather in the region (Burt 2007; Trouet et al. 2009). However, the high frequency of the time series (Figs. 10a,b) makes it difficult to characterize hydrologic drought. At longer time scales (Figs. 10c–e) EDDI clearly identifies all of the major documented hydrologic droughts over the period from 1979 to 2014 (Seager 2007; Weiss et al. 2009; McEvoy et al. 2012). The ongoing drought that began in late 2011 clearly stands out as the most severe and longest-duration event of the analyzed period. Fast recovery of hydrologic droughts are also well captured by EDDI at nearly all time scales when compared to known ''drought buster'' Prcp events (Ralph and Dettinger 2012; Dettinger 2013) and wet periods associated with El Niño (1982/83 and 1997/98) and La Niña (2010/11).

4. Discussion

Correlations of EDDI to NLDAS-2-forced drought metrics of SSI and SPI indicate that over much of CONUS, EDDI spatial distributions are generally similar to SPI and SSI. However, over parts of CONUS weak correlations were found. Comparisons of EDDI to remotely sensed ESI products also show strong correlations over much of CONUS, with the exceptions of the northeastern United States during spring and over parts of the western United States during summer. One reason for weak correlations with ESI over the northeastern United States is largely due to energy-limited land surface energy-balance conditions over the region, where ET and E_0 are often positively correlated. The two main reasons why EDDI showed weak correlations to other drought metrics are 1) that EDDI often is a leading indicator and so there is a lag present in the time series and 2) that EDDI can be strongly positive even when moisture deficits are not present on the ground but are rapidly being depleted because of high evaporative demand. It can be difficult to distinguish between drought early warning and false alarm in EDDI at short time scales, but a false alarm would only occur if soil moisture was replenished via an intense precipitation event. Our analysis highlights the advantage of using EDDI to monitor potential and actual drought development. When EDDI is used in combination with ESI, actual drought stress may be better understood. A key strength of EDDI is that it can be effectively used to provide year-round data, with no limitations during cloudy days or over snow-covered areas.

For drought monitoring in arid and semiarid regions of the western United States, EDDI aggregation to longer time scales (3–12 months) is best suited to capture the complementary relationship found between ET and E_0 (Bouchet 1963; Hobbins et al. 2004) and therefore identify and monitor extended hydrologic droughts typical of this region. Results illustrate that in most cases, when Prcp deficits at the 3–12-month time scales were fairly large, EDDI was strongly positive. The primary limitation of EDDI for hydrologic drought monitoring is that during cold droughts EDDI may not be able to capture severity because of the sensitivity to T_{air}.

5. Summary and conclusions

This work highlights an application and assessment of EDDI at multiple time scales and for several hydroclimates as a companion study to Part I. The methods and results of Part I are reinforced and a CONUS-wide evaluation is performed by examining EDDI and individual evaporative demand components as they relate to the dynamic evolution of flash drought over the central United States, characterization of hydrologic drought over the western United States, and comparison to commonly used drought metrics (USDM, SPI, SSI, and ESI). The major findings from this work are summarized as follows:

- EDDI was able to identify droughts over CONUS consistent with SPI, SSI, and ESI.
- For flash drought monitoring, EDDI showed potential development and onset of drought up to 2 months in advance of the USDM and often led SPI and SSI.
- A unique advantage of EDDI is the ability to decompose droughts and test the sensitivity of EDDI to E_0 drivers. High U and low q played a major role in initiating the 2011 flash drought case in Iowa. This was followed by extreme positive T_{air} anomalies that drove much of the EDDI drought signal in 2012 and exacerbated the depletion of SM.
- Tracking drought using submonthly data and multiple drought indices (Fig. 8) can add value to operational drought monitoring relative to simply using monthly data. Flash droughts are dynamic, with large changes in moisture availability possible over a 1-month period, even when considering a time series run through a 30-day smoothing filter (i.e., a 1-month drought index time scale).
- Despite being independent of precipitation, EDDI is able to capture long-term hydrologic and snow drought in the western United States.

Despite some limitations, EDDI is shown to provide useful information on the less understood and documented dynamical processes associated with drought evolution and persistence. Results highlighted in this work illustrate the benefits of assimilating physically based E_0 estimates and EDDI into operational monitoring

products such as the USDM. The additional information and early warning provided by EDDI could greatly contribute to a stronger understanding of drought evolution and dynamics, land surface–atmosphere interactions, and, perhaps more importantly, reduce and/or mitigate future adverse societal effects that have been associated with past droughts. EDDI could also prove useful and effective for easy-to-implement operational early warning for agricultural and fire-weather monitoring (Ham et al. 2014) and seasonal forecasting of drought (McEvoy et al. 2016).

Acknowledgments. The NLDAS-2 data were acquired as part of the mission of NASA's Earth Science Division and archived and distributed by the Goddard Earth Sciences (GES) Data and Information Services Center (DISC). Dr. Hobbins was supported from the National Integrated Drought Information System (NIDIS) and from an Inter-Agency Agreement between the U.S. Agency for International Development (USAID) and NOAA for support to the Famine Early Warning Systems Network (FEWS NET; AID-FFP-P-10-00002/006). Dr. Wood was supported by a NOAA MAPP Grant (NA11OAR4310142). Dr. McEvoy, Dr. Huntington, and Mr. Morton were supported by a DRI Maki Endowment for Enhancing Water Resource Monitoring in Southern Nevada Grant (6223-640-0969), a U.S. Bureau of Reclamation Climate Analysis Tools WaterSMART Program Grant (R11AP81454), a U.S. Geological Survey and DRI Great Basin Cooperative Ecosystem Study Unit Collaborative Project on Drought Monitoring and Fallow Field-Tracking through Cloud Computing of Landsat, MODIS, and Gridded Climate Data Archives Grant (G15AC00137), and a U.S. Bureau of Land Management Grant (L13AC00169). Dr. Anderson and Dr. Hain were supported by a NASA Applied Sciences Water Resources Grant (NNX12AK90G).

REFERENCES

Abatzoglou, J. T., 2013: Development of gridded surface meteorological data for ecological applications and modelling. *Int. J. Climatol.*, **33**, 121–131, doi:10.1002/joc.3413.

——, R. Barbero, J. Wolf, and Z. Holden, 2014: Tracking interannual streamflow variability with drought indices in the U.S. Pacific Northwest. *J. Hydrometeor.*, **15**, 1900–1912, doi:10.1175/JHM-D-13-0167.1.

Allen, R. G., I. A. Walter, R. Elliott, T. Howell, D. Itenfisu, and M. Jensen, 2005: The ASCE standardized reference evapotranspiration equation. Rep. 0-7844-0805-X, 59 pp. [Available online at http://www.kimberly.uidaho.edu/water/asceewri/ascestzdetmain2005.pdf.]

Anderson, M. C., J. M. Norman, G. R. Diak, W. P. Kustas, and J. R. Mecikalski, 1997: A two-source time-integrated model for estimating surface fluxes using thermal infrared remote sensing. *Remote Sens. Environ.*, **60**, 195–216, doi:10.1016/S0034-4257(96)00215-5.

——, ——, J. R. Mecikalski, J. A. Otkin, and W. P. Kustas, 2007a: A climatological study of evapotranspiration and moisture stress across the continental United States based on thermal remote sensing: 1. Model formulation. *J. Geophys. Res.*, **112**, D10117, doi:10.1029/2006JD007506.

——, ——, ——, ——, and ——, 2007b: A climatological study of evapotranspiration and moisture stress across the continental United States based on thermal remote sensing: 2. Surface moisture climatology. *J. Geophys. Res.*, **112**, D11112, doi:10.1029/2006JD007507.

——, C. Hain, B. Wardlow, A. Pimstein, J. R. Mecikalski, and W. P. Kustas, 2011: Evaluation of drought indices based on thermal remote sensing of evapotranspiration over the continental United States. *J. Climate*, **24**, 2025–2044, doi:10.1175/2010JCLI3812.1.

——, ——, J. Otkin, X. Zhan, K. Mo, M. Svoboda, B. Wardlow, and A. Pimstein, 2013: An intercomparison of drought indicators based on thermal remote sensing and NLDAS-2 simulations with U.S. Drought Monitor classifications. *J. Hydrometeor.*, **14**, 1035–1056, doi:10.1175/JHM-D-12-0140.1.

Bouchet, R. J., 1963: Évapotranspiration réelle et potentielle, signification climatique. *IAHS Publ.*, **62**, 134–142.

Burt, C. C., 2007: *Extreme Weather: A Guide and Record Book*. W. W. Norton and Co., 320 pp.

Cattiaux, J., and P. Yiou, 2013: U.S. heat waves of spring and summer 2012 from the flow-analogue perspective [in "Explaining Extreme Events of 2012 from a Climate Perspective"]. *Bull. Amer. Meteor. Soc.*, **94**, S10–S13, doi:10.1175/BAMS-D-12-00021.1.

Dai, A., 2011: Characteristics and trends in various forms of the Palmer drought severity index during 1900–2008. *J. Geophys. Res.*, **116**, D12115, doi:10.1029/2010JD015541.

Daly, C., R. P. Neilson, and D. L. Phillips, 1994: A statistical–topographic model for mapping climatological precipitation over mountainous terrain. *J. Appl. Meteor.*, **33**, 140–158, doi:10.1175/1520-0450(1994)033<0140:ASTMFM>2.0.CO;2.

Dettinger, M. D., 2013: Atmospheric rivers as drought busters on the U.S. West Coast. *J. Hydrometeor.*, **14**, 1721–1732, doi:10.1175/JHM-D-13-02.1.

Farahmand, A., and A. AghaKouchak, 2015: A generalized framework for deriving nonparametric standardized indicators. *Adv. Water Resour.*, **76**, 140–145, doi:10.1016/j.advwatres.2014.11.012.

Guttman, N. B., 1999: Accepting the Standardized Precipitation Index: A calculation algorithm. *J. Amer. Water Resour. Assoc.*, **35**, 311–322, doi:10.1111/j.1752-1688.1999.tb03592.x.

Ham, C., M. T. Hobbins, K. L. Abt, and J. P. Prestemon, 2014: Using the Evaporative Demand Drought Index and the Palmer drought severity index to forecast the number of large wildland fires on federal lands. *Large Wildland Fires Conf.*, Missoula, MT, Association for Fire Ecology and the International Association of Wildland Fire. [Available online at http://largefireconference.org/wp-content/uploads/2013/06/Oral-Presentation-Abstracts-V4.pdf.]

Han, S., F. Tian, and H. Hu, 2014: Positive or negative correlation between actual and potential evaporation? Evaluating using a nonlinear complementary relationship model. *Water Resour. Res.*, **50**, 1322–1336, doi:10.1002/2013WR014151.

Hao, Z., and A. AghaKouchak, 2014: A nonparametric multivariate multi-index drought monitoring framework. *J. Hydrometeor.*, **15**, 89–101, doi:10.1175/JHM-D-12-0160.1.

Hargreaves, G. H., and Z. A. Samani, 1985: Reference crop evapotranspiration from temperature. *Appl. Eng. Agric.*, **1**, 96–99, doi:10.13031/2013.26773.

Heddinghaus, T. R., and P. Sabol, 1991: A review of the Palmer drought severity index and where do we go from here? Preprints, *Seventh Conf. on Applied Climatology*, Boston, MA, Amer. Meteor. Soc., 242–246.

Hobbins, M. T., 2016: The variability of ASCE standardized reference evapotranspiration: A rigorous, CONUS-wide decomposition and attribution. *Trans. ASABE*, **59**, 561–576, doi:10.13031/trans.59.10975.

——, J. A. Ramírez, and T. C. Brown, 2004: Trends in pan evaporation and actual evaporation across the conterminous U.S.: Paradoxical or complementary? *Geophys. Res. Lett.*, **31**, L13503, doi:10.1029/2004GL019846.

——, A. Dai, M. L. Roderick, and G. D. Farquhar, 2008: Revisiting the parameterization of potential evaporation as a driver of long-term water balance trends. *Geophys. Res. Lett.*, **35**, L12403, doi:10.1029/2008GL033840.

——, A. Wood, D. Streubel, and K. Werner, 2012: What drives the variability of evaporative demand across the conterminous United States? *J. Hydrometeor.*, **13**, 1195–1214, doi:10.1175/JHM-D-11-0101.1.

——, ——, D. J. McEvoy, J. L. Huntington, C. Morton, and J. Verdin, 2016: The Evaporative Demand Drought Index. Part I: Linking drought evolution to variations in evaporative demand. *J. Hydrometeor.*, **17**, 1745–1761, doi:10.1175/JHM-D-15-0121.1.

Jensen, M. E., 1973: *Consumptive Use of Water and Irrigation Water Requirements*. American Society of Civil Engineers, 215 pp.

Karl, T. R., and Coauthors, 2012: U.S. temperature and drought: Recent anomalies and trends. *Eos, Trans. Amer. Geophys. Union*, **93**, 473–474, doi:10.1029/2012EO470001.

Koster, R. D., and Coauthors, 2004: Regions of strong coupling between soil moisture and precipitation. *Science*, **305**, 1138–1140, doi:10.1126/science.1100217.

——, and Coauthors, 2006: GLACE: The Global Land–Atmosphere Coupling Experiment. Part I: Overview. *J. Hydrometeor.*, **7**, 590–610, doi:10.1175/JHM510.1.

——, S. D. Schubert, and M. J. Suarez, 2009: Analyzing the concurrence of meteorological droughts and warm periods, with implications for the determination of evaporative regime. *J. Climate*, **22**, 3331–3341, doi:10.1175/2008JCLI2718.1.

Liang, X., D. P. Lettenmaier, E. F. Wood, and S. J. Burges, 1994: A simple hydrologically based model of land surface water and energy fluxes for general circulation models. *J. Geophys. Res.*, **99**, 14 415–14 428, doi:10.1029/94JD00483.

McEvoy, D. J., J. L. Huntington, J. T. Abatzoglou, and L. M. Edwards, 2012: An evaluation of multiscalar drought indices in Nevada and eastern California. *Earth Interact.*, **16**, doi:10.1175/2012EI000447.1.

——, ——, J. F. Mejia, and M. T. Hobbins, 2016: Improved seasonal drought forecasts using reference evapotranspiration anomalies. *Geophys. Res. Lett.*, **43**, 377–385, doi:10.1002/2015GL067009.

McKee, T. B., N. J. Doesken, and J. Kleist, 1993: The relationship of drought frequency and duration to time scales. Preprints, *Eighth Conf. on Applied Climatology*, Anaheim, CA, Amer. Meteor. Soc., 179–184.

Mesinger, F., and Coauthors, 2006: North American Regional Reanalysis. *Bull. Amer. Meteor. Soc.*, **87**, 343–360, doi:10.1175/BAMS-87-3-343.

Milly, P. C. D., and K. A. Dunne, 2011: On the hydrologic adjustment of climate-model projections: The potential pitfall of potential evapotranspiration. *Earth Interact.*, **15**, doi:10.1175/2010EI363.1.

Mo, K. C., and D. P. Lettenmaier, 2015: Heat wave flash droughts in decline. *Geophys. Res. Lett.*, **42**, 2823–2829, doi:10.1002/2015GL064018.

Monteith, J. L., 1965: Evaporation and environment. *Symp. Soc. Exp. Biol.*, **19**, 205–234.

Mu, Q., M. Zhao, J. S. Kimball, N. G. McDowell, and S. W. Running, 2013: A remotely sensed global terrestrial drought severity index. *Bull. Amer. Meteor. Soc.*, **94**, 83–98, doi:10.1175/BAMS-D-11-00213.1.

Otkin, J. A., M. C. Anderson, C. Hain, I. E. Mladenova, J. B. Basara, and M. Svoboda, 2013: Examining rapid onset drought development using the thermal infrared–based evaporative stress index. *J. Hydrometeor.*, **14**, 1057–1074, doi:10.1175/JHM-D-12-0144.1.

——, ——, ——, and M. Svoboda, 2014: Examining the relationship between drought development and rapid changes in the evaporative stress index. *J. Hydrometeor.*, **15**, 938–956, doi:10.1175/JHM-D-13-0110.1.

Palmer, W. C., 1965: Meteorological drought. U.S. Weather Bureau Research Paper 45, 58 pp. [Available online at http://www.ncdc.noaa.gov/temp-and-precip/drought/docs/palmer.pdf.]

Priestley, C. H. B., and R. J. Taylor, 1972: On the assessment of surface heat flux and evaporation using large-scale parameters. *Mon. Wea. Rev.*, **100**, 81–92, doi:10.1175/1520-0493(1972)100<0081:OTAOSH>2.3.CO;2.

Quiring, S. M., 2009: Developing objective operational definitions for monitoring drought. *J. Appl. Meteor. Climatol.*, **48**, 1217–1229, doi:10.1175/2009JAMC2088.1.

Ralph, F. M., and M. D. Dettinger, 2012: Historical and national perspectives on extreme West Coast precipitation associated with atmospheric rivers during December 2010. *Bull. Amer. Meteor. Soc.*, **93**, 783–790, doi:10.1175/BAMS-D-11-00188.1.

Roderick, M. L., M. T. Hobbins, and G. D. Farquhar, 2009: Pan evaporation trends and the terrestrial water balance. II. Energy balance and interpretation. *Geogr. Compass*, **3**, 761–780, doi:10.1111/j.1749-8198.2008.00214.x.

Seager, R., 2007: The turn of the century North American drought: Global context, dynamics, and past analogs. *J. Climate*, **20**, 5527–5552, doi:10.1175/2007JCLI1529.1.

——, M. Hoerling, S. Schubert, H. Wang, B. Lyon, A. Kumar, J. Nakamura, and N. Henderson, 2015: Causes of the 2011–14 California drought. *J. Climate*, **28**, 6997–7024, doi:10.1175/JCLI-D-14-00860.1.

Sheffield, J., E. F. Wood, and M. L. Roderick, 2012: Little change in global drought over the past 60 years. *Nature*, **491**, 435–438, doi:10.1038/nature11575.

Svoboda, M., and Coauthors, 2002: The Drought Monitor. *Bull. Amer. Meteor. Soc.*, **83**, 1181–1190, doi:10.1175/1520-0477(2002)083<1181:TDM>2.3.CO;2.

Thornthwaite, C. W., 1948: An approach toward a rational classification of climate. *Geogr. Rev.*, **38**, 55–94, doi:10.2307/210739.

Trouet, V., A. H. Taylor, A. M. Carleton, and C. N. Skinner, 2009: Interannual variations in fire weather, fire extent, and synoptic-scale circulation patterns in Northern California and Oregon. *Theor. Appl. Climatol.*, **95**, 349–360, doi:10.1007/s00704-008-0012-x.

van der Schrier, G., P. D. Jones, and K. R. Briffa, 2011: The sensitivity of the PDSI to the Thornthwaite and Penman–Monteith

parameterizations for potential evapotranspiration. *J. Geophys. Res.*, **116**, D03106, doi:10.1029/2010JD015001.

Vicente-Serrano, S. M., J. I. López-Moreno, S. Beguería, J. Lorenzo-Lacruz, C. Azorin-Molina, and E. Morán-Tejeda, 2012: Accurate computation of a streamflow drought index. *J. Hydrol. Eng.*, **17**, 318–332, doi:10.1061/(ASCE)HE.1943-5584.0000433.

Weiss, J. L., C. L. Castro, and J. T. Overpeck, 2009: Distinguishing pronounced droughts in the southwestern United States: Seasonality and effects of warmer temperatures. *J. Climate*, **22**, 5918–5932, doi:10.1175/2009JCLI2905.1.

Xia, Y., and Coauthors, 2012a: Continental-scale water and energy flux analysis and validation for the North American Land Data Assimilation System project phase 2 (NLDAS-2): 1. Intercomparison and application of model products. *J. Geophys. Res.*, **117**, D03109, doi:10.1029/2011JD016048.

——, and Coauthors, 2012b: Continental-scale water and energy flux analysis and validation for the North American Land Data Assimilation System project phase 2 (NLDAS-2): 2. Validation of model-simulated streamflow. *J. Geophys. Res.*, **117**, D03110, doi:10.1029/2011JD016051.

Yao, Y., S. Liang, Q. Qin, and K. Wang, 2010: Monitoring drought over the conterminous United States using MODIS and NCEP Reanalysis-2 data. *J. Appl. Meteor. Climatol*, **49**, 1665–1680, doi:10.1175/2010JAMC2328.1.